J Mater Sci: Mater Electron (2017) 28:1–9
DOI 10.1007/s10854-016-5486-1

Preparation and characterization of various morphologies of $SrFe_{12}O_{19}$ nano-structures: investigation of magnetization and coercivity

Kambiz Hedayati[1] · Zahra Behesht-Ara[1] · Davood Ghanbari[2]

Received: 2 July 2016 / Accepted: 1 August 2016 / Published online: 5 August 2016

Abstract Hard magnetic $SrFe_{12}O_{19}$ (SrFe) nanostructures were synthesized by a facile chemical precipitation procedure. The influence of temperature, concentration and different capping agents on the particle size and morphology of the magnetic nanoparticles was investigated. The synthesized ferrites were characterized by X-ray diffraction pattern, scanning electron microscope, and Fourier transform infrared spectroscopy. Ferromagnetic property of the hexaferrite nanostructures was determined by vibrating sample magnetometer. The results show hard magnetic ferrite with a high coercivity about 2800–4000 Oe and saturation magnetization around 11–14 emu/g were synthesized.

1 Introduction

Ferrites are of ceramic materials belong to transition metals group combined with oxygen in which iron oxide is of the most important components [1]. Compared with spinel ferrite, magnetoplumbite ferrites, strontium hexa ferrite have attracted more scientific research in recent years due to their high uniaxial magnetic anisotropy, high saturation magnetization and high coercivity in multidisciplinary areas including physics, spintronics, biomedicine and materials science. These combinations are used in chemical photocells, ceramic glazes, generators, motors and transformers to produce high magnetic flux [2]. Several techniques have been used to prepare strontium ferrites such as ball milling [3], salt melting [4], chemical precipitation [5], glass crystallization [6] micro emulsion, and citrate precursor [7] and self propagating high temperature synthesis [8] to prepare intrinsic and doped hexagonal ferrite for high-density magnetic media and microwave devices [9, 10]. However, most of these methods cannot be economically applied on a large scale because they need expensive and often toxic reagents, complicated synthetic steps, high temperatures and long times. This not only results in waste of energy but also harms our environment. These routes require prolonged thermal treatment to improve the crystallinity, purity, and morphology of the powders. Hence a chemical route can be excellent method for the synthesis of highly pure multi-component oxide due to its simplicity, suitable-control grain size, homogeneity, compositional control and lower processing temperatures which are some advantages of this wet chemical method over the conventional solid state reaction route [11]. Sol–gel technique has been applied to barium and strontium ferrite, with the advantage of the chemical route of a lower annealing temperature necessary in the crystallization process [12, 13]. Now, ferrite powders are manufactured for dielectric and magnetic ceramic devices. Ceramic powders have been acquired by calcination. Mixed oxides with spinel structure (e.g. ferrites) are also made in a calcination process [14]. Simple production, affordable price, and suitable application also motivate the using of these

✉ Kambiz Hedayati
K-hedayati@arakut.ac.ir

[1] Department of Science, Arak University of Technology, Arak, Iran

[2] Young Researchers and Elite Club, Arak Branch, Islamic Azad University, Arak, Iran

materials in applied microwave devices [15]. Ferrites are divided into three categories; soft ferrites as spinels, hard ferrites as hexa ferrites and garnets. Hexagonal ferrites $MFe_{12}O_{19}$ (M = Ba, Sr, Pb,.) with a magnetoplumbite structure type are widely used for technological applications. In particular strontium hexa-ferrite is used for its hard magnetic properties. The strontium ferrite is wide applied in permanent magnetic material as a result of the following advantages: raw material is abundant, the manufacture cost is low, the properties are stable and the sample cannot be oxygenated. Their importance arises from their unique and tuneable magnetic, electronic and structural properties [16–21].

2 Experimental

2.1 Materials and methods

$Sr(NO_3)_2$, $SrCl_2 \cdot 6H_2O$, $Fe(NO_3)_3 \cdot 9H_2O$, NaOH were purchased from Merck and all the chemicals were used as received without further purifications. A multi-wave ultrasonic generator (Bandeline MS 73), equipped with a converter/transducer and titanium oscillator, operating at 20 kHz with a maximum power output of 150 W was used for the ultrasonic irradiation. Room temperature magnetic properties were investigated using a vibrating sample magnetometer (VSM) device, made by Meghnatis Kavir Kashan Company (Iran) in an applied magnetic field sweeping between ±10,000 Oe. XRD patterns were recorded by a Philips, X-ray diffractometer using Ni-filtered CuK_α radiation. SEM images were obtained using a LEO instrument model 1455VP. Prior to taking images, the samples were coated by a very thin layer of Pt (using a BAL-TEC SCD 005 sputter coater) to make the sample surface conductor and prevent charge accumulation, and obtaining a better contrast.

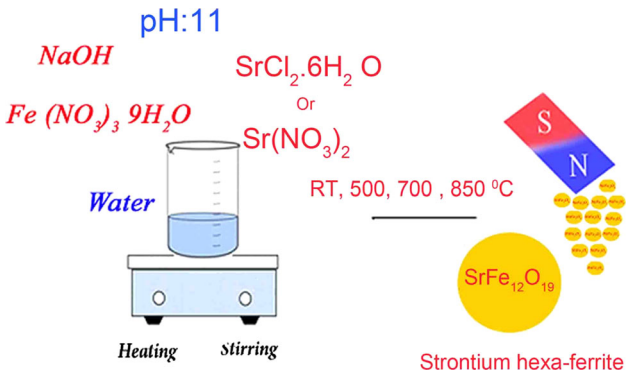

Fig. 1 Chemical preparation of nanoparticles

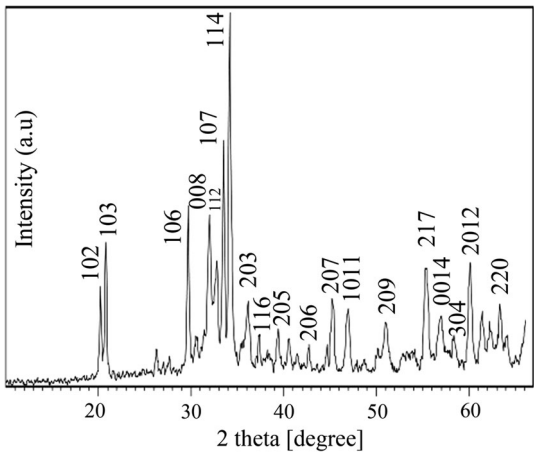

Fig. 2 XRD pattern of strontium ferrite nanoparticles

2.2 Preparation of magnetic nanostructure

0.001 mol of $SrCl_2 \cdot 6H_2O$ (or $Sr(NO_3)_2$) and 0.012 mol of $Fe(NO_3)_3 \cdot 9H_2O$ were dissolved in 100 ml water and put on the on magnetic stirrer for 15 min was stirred until materials were completely dissolved. Then 30 ml of NaOH solution (1 M) was slowly added, until reaching pH to

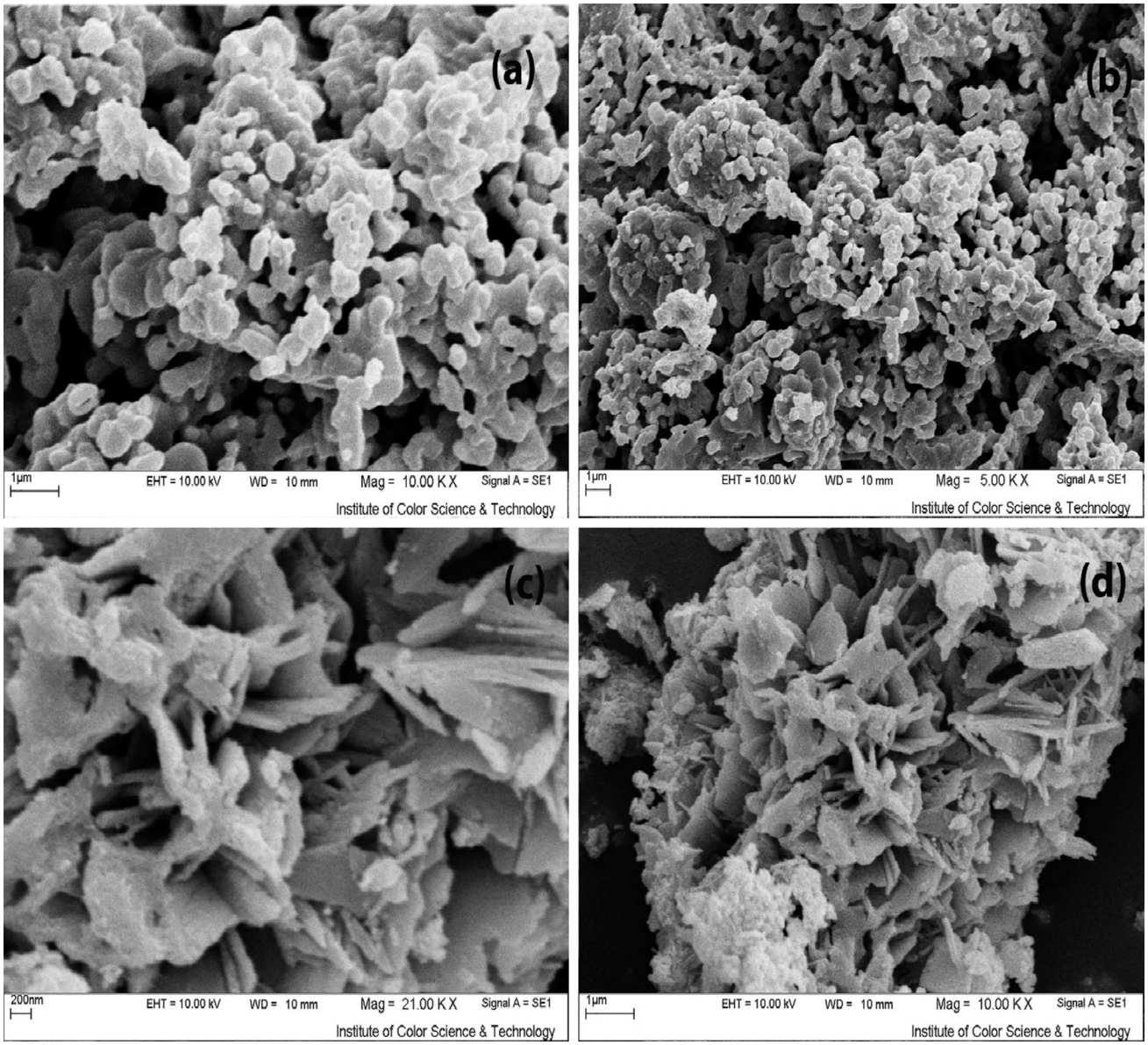

Fig. 3 SEM image of product prepared by **a**, **b** $SrCl_2$, 700 °C, **c**, **d** $Sr(NO_3)_2$, 500 °C

around 10. Slowly return the colour to brown. Solution turned for half hour and then was abandoned for a time to precipitate. The remaining sediment was centrifuged and was placed inside the oven at 80 °C. Then some of the products were calcinated at 700 °C for 2 h (Fig. 1).

3 Results and discussion

Figure 2 shows XRD pattern of sample including $SrFe_{12}O_{19}$ nanoparticles. The structure and composition of the $SrFe_{12}O_{19}$ nanoparticles was investigated. The XRD pat-

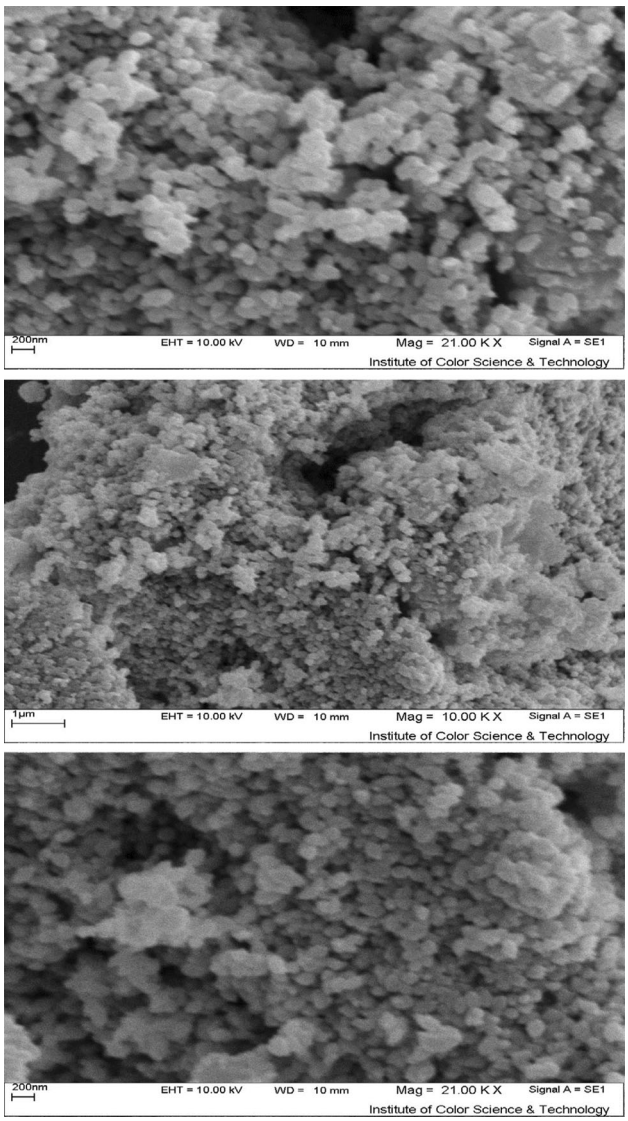

Fig. 4 SEM image of product prepared by $Sr(NO_3)_2$, 850 °C, 4 h, 100 ml

tern of ferrite reveals the typical diffraction pattern of hexagonal phase (JCPDS No.: 24-1207) with P63-mmc space group which has agreement with strontium hexa-ferrite. The calculated crystalline sizes from Scherrer equation, $D_c = K\lambda/\beta Cos\theta$, where β is the width of the observed diffraction peak at its half maximum intensity (FWHM), K is the shape factor, which takes a value of about 0.9, and λ is the X-ray wavelength (CuK_α radiation, equals to 0.154 nm) was about 28 nm for $SrFe_{12}O_{19}$ nanoparticles.

Figure 3a, b show Scanning Electron Microscopy image of product prepared by $SrCl_2$ at 700 °C for 2 h, the results confirm preparation of nano structures with average particle size about 150 nm. SEM image of strontium ferrite synthesized by $Sr(NO_3)_2$ at 500 °C for 4 h are shown in Fig. 3c, d, the images approve formation of flower-like nano structures which diameter of nano-plate are less than 100 nm. It seems in this reaction growth stage is predominant compare to nucleation stage and as a result preferential growth was observed.

The effect of temperature on the morphology and particle size was investigated, Fig. 4 illustrate SEM image of hexa-ferrite that where obtained by $Sr(NO_3)_2$ at 850 °C for 4 h. Mono-disperse nanoparticles with average size around 70 nm where achieved. The outcomes show that in lower temperature smaller nanoparticles were prepared.

The influence of concentration and temperature on the shape and size of product was also examined, and amount of water was increased from 100 to 250 ml. Figure 5a, b depict SEM image of magnetic strontium ferrite prepared without calcination by $Sr(NO_3)_2$ in 250 ml. Gelatine as a green, bio-compatible and bio-degradable capping agent was used and images of hard magnetic by $Sr(NO_3)_2$ precursor in 250 ml of water are illustrated in Fig. 5c, d, outcomes approve agglomerated nano structures with mediocre size about 100 nm were formed.

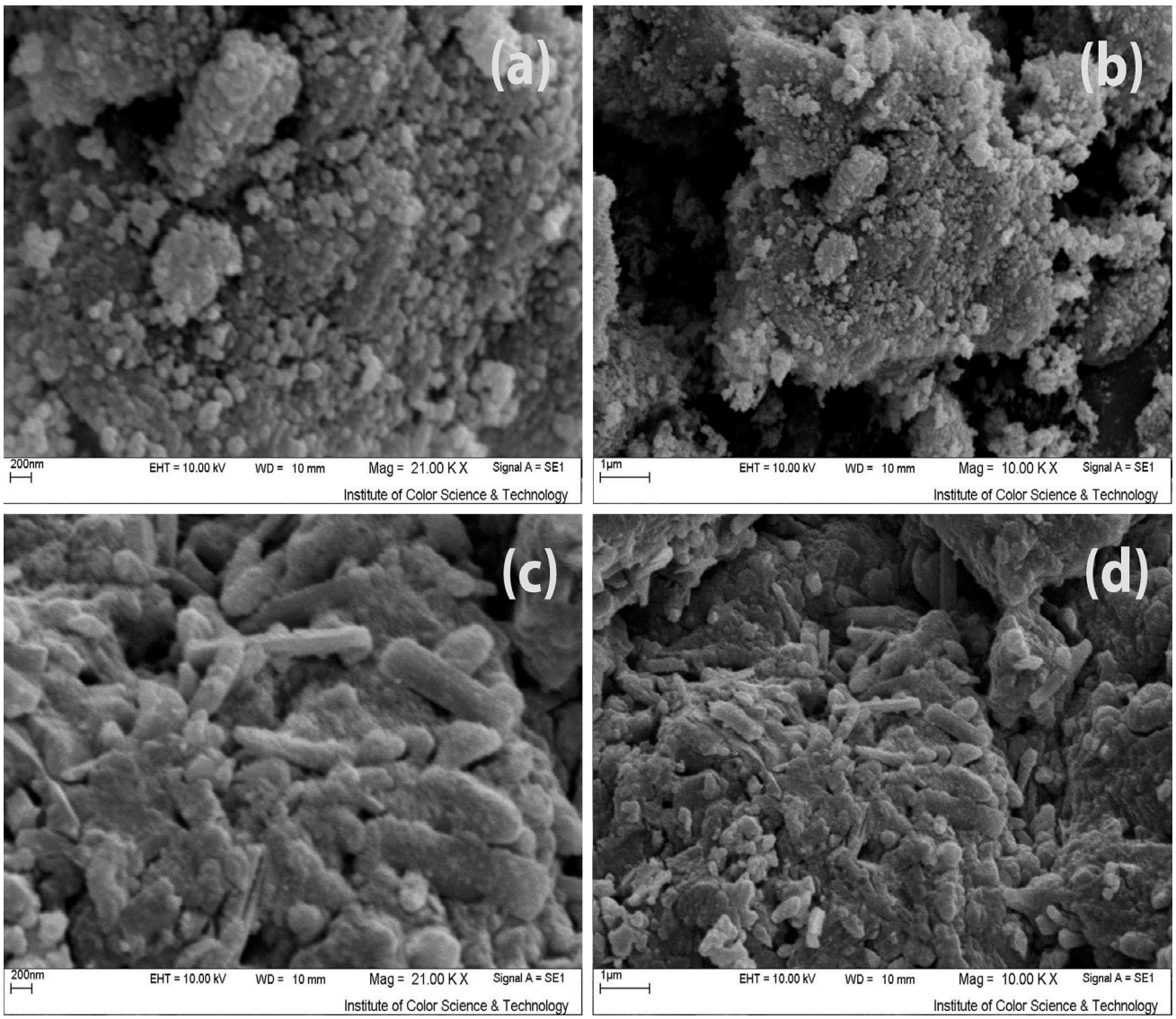

Fig. 5 SEM image of product prepared by **a**,**b** $Sr(NO_3)_2$, 250 ml of water, **c**, **d** $Sr(NO_3)_2$, gelatine, 250 ml of water

Starch as another green and cost effective carbohydrate was added to the solution and effect of this bio-polymer on the morphology and crystal size was investigated. Figure 6a, b show $SrFe_{12}O_{19}$ prepared at presence of starch calcinated at 700 °C for 2 h, according to SEM images disorder hexagonal plates were observed. SEM image of product prepared by $SrCl_2$ precursor at 700 °C for 2 h by adding gelatine is shown in Fig. 6c. Nano particles with average particle size around 100 nm were synthesized.

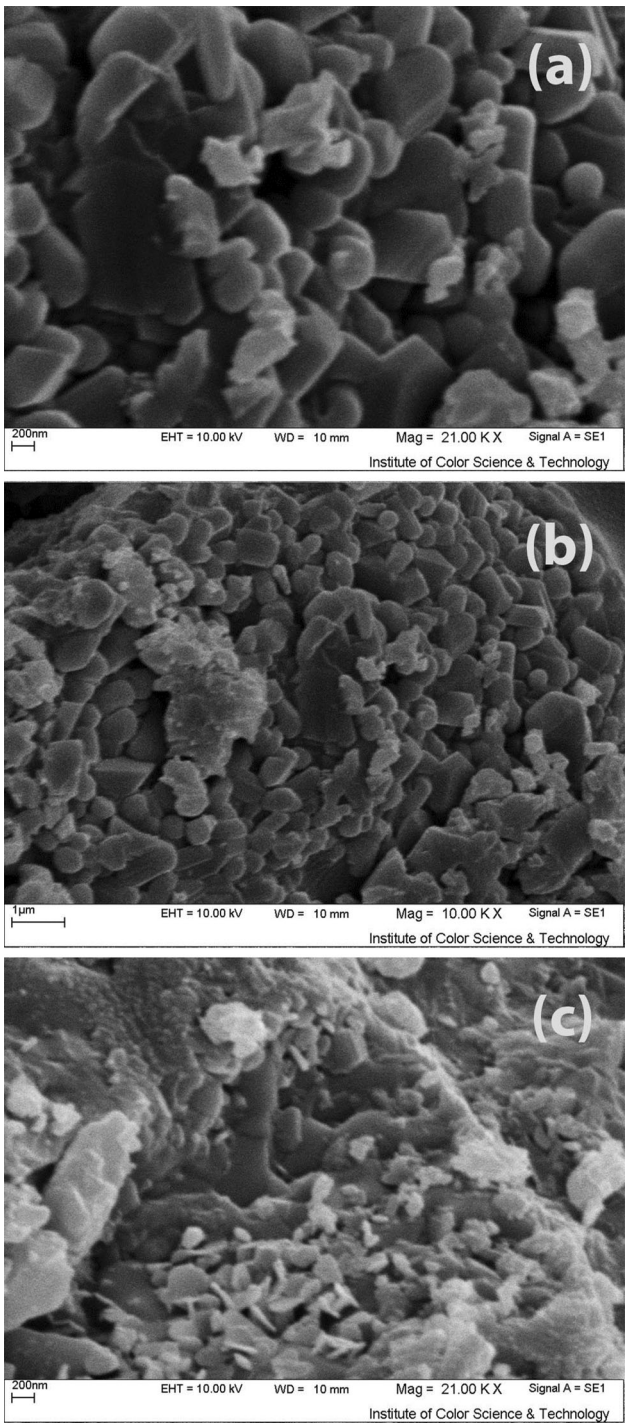

Fig. 6 SEM images of product presented by **a**, **b** $SrCl_2$, 700, 2 h, Starch, 100 ml, **c** $SrCl_2$, 700, 2 h, gelatin, 100 ml

The influence polyvinyl pyrrolidone as a neutral surfactant and capping agent on the size and configuration was surveyed Fig. 7 illustrate PVP effect at presence different strontium precursor. Figure 7a, b show SEM image of product prepared by $SrCl_2$ precursor and Fig. 7c, d show image obtained by $Sr(NO_3)_2$, precursor respectively. The results approve nitrate precursor leads to smaller nanoparticles, in comparison to chloride salt.

Figure 8 show SEM image of product obtained by strontium nitrate at 700 °C and 2 h at presence of gelatine, it seems by reaction of gelatine with nitrate the most monodisperse and spherical magnetic nano-structures with average size around 100 nm were achieved.

Figure 9 shows the FT-IR spectrum of the $SrFe_{12}O_{19}$ nanoparticles at 500 °C, the absorption peaks at 450 and 553 cm^{-1} are responsible to the stretching mode of Fe–O and Sr–O bonds. FT-IR spectrum of nanoparticle clearly shows metal–oxygen bonds around 300-600 cm^{-1}. The spectrum exhibits broad absorption peaks between 3500 and 3500 cm^{-1}, corresponding to the stretching mode of O–H group of hydroxyl group and the weak band near 1456 cm^{-1} is assigned to H–O–H bending vibration mode due to the adsorption of moisture on the surface of nanoparticles [19]. FT-IR spectrum of the $SrFe_{12}O_{19}$ nanoparticles calcinated at 850 °C is shown in Fig. 10 the absorptions peak at 340, 448 and 565 cm^{-1} are responsible to the stretching mode of Fe–O and Sr–O bonds.

Room temperature magnetic property of samples was studied using vibrating sample magnetometer (VSM) device and is shown in Fig. 11 at 500 °C. The results confirm preparation of a hard ferro magnetic with a high coercivity about 2750 Oe and saturation magnetization around 11.3 emu/g.

Hysteresis loop for $SrFe_{12}O_{19}$ magnetite nanoparticles in 700 °C is shown in Fig. 12. Interestingly it was observed at higher temperature coercivity is higher than 500 °C. The outcomes show the direct effect of temperature on the magnetic property of the prepared ferrite. Saturation magnetization is also so higher than 500 °C and it is around 12.1 emu/g with a high coercivity about 3470 Oe.

Figure 13 shows magnetization curve of $SrFe_{12}O_{19}$ calcinated at 850 °C that exhibits ferromagnetic behaviour with a higher coercivity compare to other samples. Coercivity is near 4000 Oe and saturation magnetization is 14.4 emu/g.

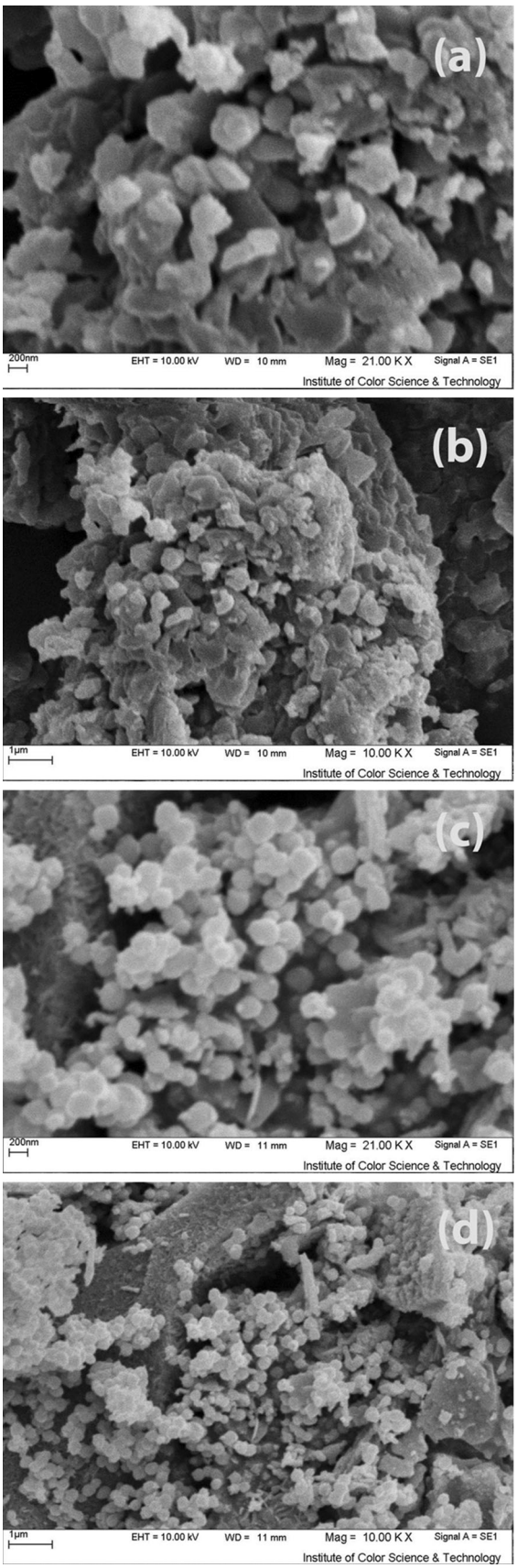

◄**Fig. 7** SEM images of product prepared by (a,b) $SrCl_2$, PVP (c,d) $Sr(NO_3)_2$, PVP

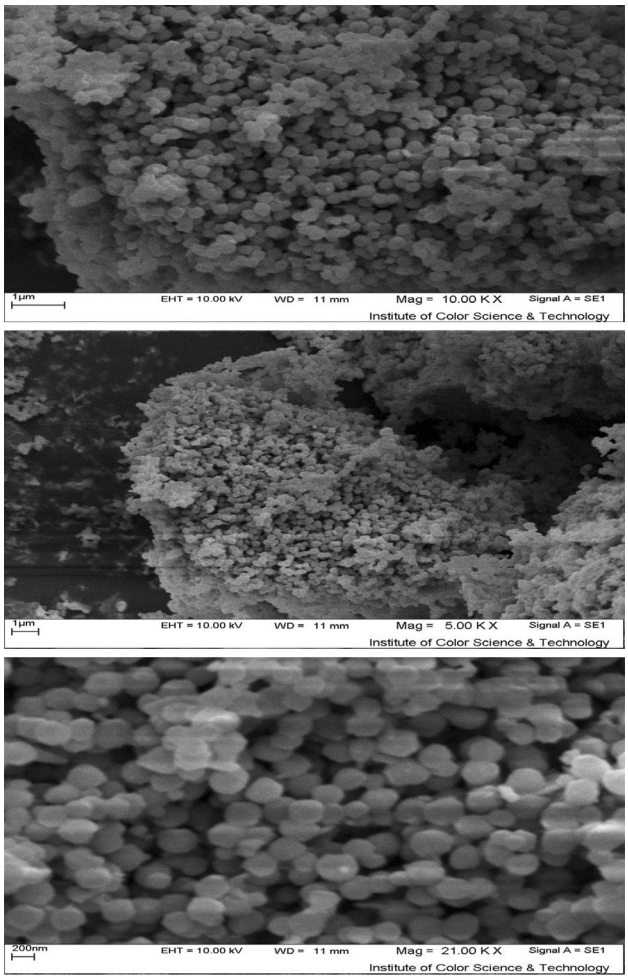

Fig. 8 SEM images of product obtained by $Sr(NO_3)_2$, gelatine

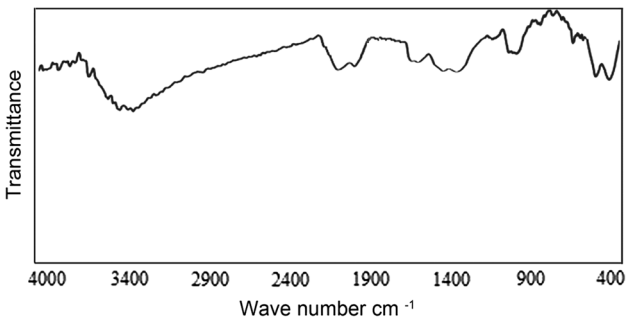

Fig. 9 FT-IR spectrum of nanoparticles obtained at 500 °C

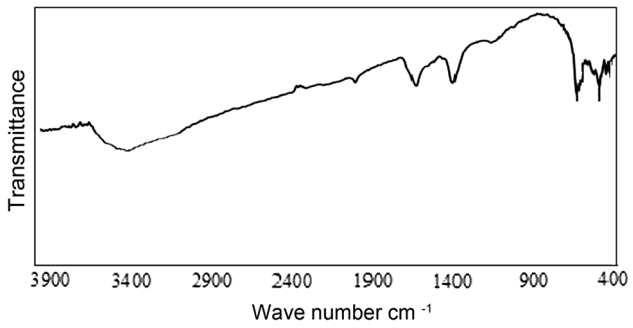

Fig. 10 FT-IR spectrum of nanoparticles obtained at 850 °C

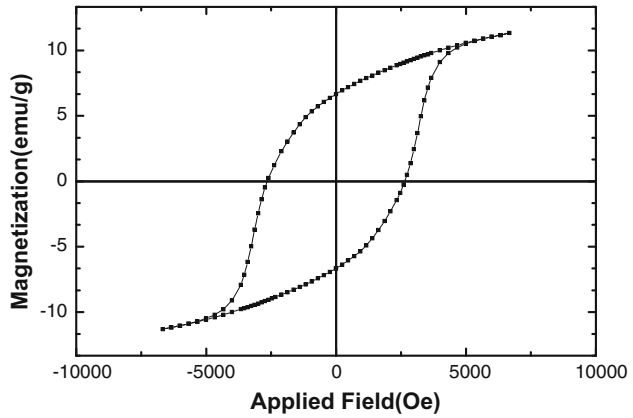

Fig. 11 Room temperature hysteresis loop achieved at 500 °C

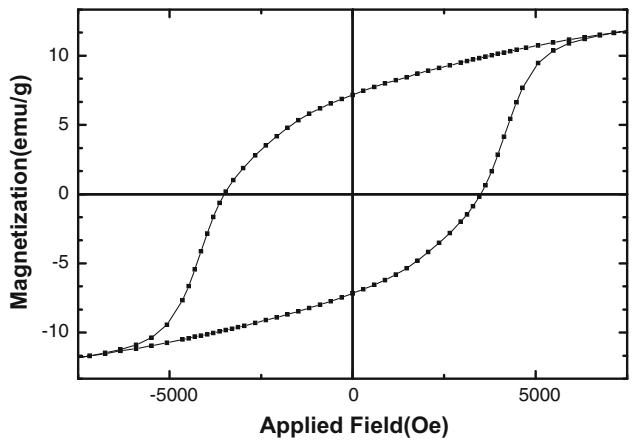

Fig. 12 Room temperature hysteresis loop obtained at 700 °C

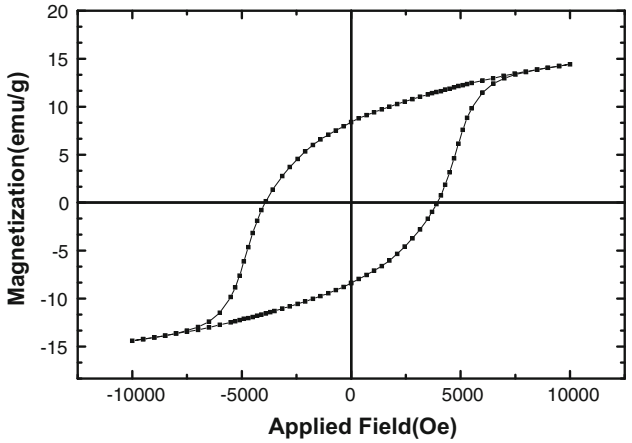

Fig. 13 Hysteresis loop of ferrite calcinated at 850 °C

4 Conclusions

In conclusion, synthesis, characterization, and magnetic activity of $SrFe_{12}O_{19}$ nanocomposite was reported. Effect of temperature, precursor, concentration and various surfactants and capping agents on the morphology and particle size of the products was investigated. AGFM confirmed that nanoparticles at different temperatures exhibit ferromagnetic behaviour applicable as hard magnetic materials.

References

1. C.B. Carter, M.G. Norton, *Ceram Mater* (Springer, New York, 2007)
2. L.G.J. Haart, G. Blasee, Solid State Ion. **16**, 137–140 (1985)
3. W.A. Kazamareck, B. Idikowski, K.H. Muller, J. Magn. Magn. Mater. **921**, 177–181 (1998)
4. Z.B. Guo, W.P. Ding, W. Zhong, J.R. Zang, Y.W. Do, J. Magn. Magn. Mater. **175**, 333–336 (1997)
5. A. Ataie, S. Heshmati-Manesh, J. Eur. Ceram. Soc. **21**, 1951–1955 (2001)
6. H. Sato, T. Umeda, J. Mater. Trans. **34**, 76–81 (1993)
7. K. Samikannu, J. Sinnappan, S. Mannarswamy, T. Cinnasamy, K. Thirunavukarasu, J. Mater. Sci. **2**, 6 (2011)
8. G. Elvin, I.P.P. Parkin, Q.T. Bui, L. Fernandez Barquin, Q.A. Pankhurst, A.V. Komarov, Y.G. Morozov, J. Mater. Sci. Lett. **16**, 1237 (1997)
9. C. Surrig, K.A. Hempel, D. Bonnenberg, Appl. Phys. Lett. **63**, 1836 (1993)

10. R. Nawathey-Dikshit, S.R. Shinde, S.B. Ogale, Appl. Phys. Lett. **68**, 3491 (1996)
11. M. Kakihana, J. Sol-Gel. Sci. Technol. **6**, 5 (1996)
12. R. Carey, P.A. Gago-Sandocal, D.M. Newman, B.W.J. Thomas, J. Appl. Phys. **75**, 6789 (1994)
13. Q.Q. Fang, W. Zhong, Y.W. Du, Chin. Phys. Lett. **16**, 285 (1999)
14. V. Hlavacek, J.A. Puszynski, J. Ind. Eng. Chem. Res. **35**, 349 (1996)
15. M. Pardavi-Horvath, J. Magn. Magn. Mater. **215**, 171 (2000)
16. H. Halakouie, G. Nabiyouni, J. Saffari, A. Ahmadi, D. Ghanbari, J. Mater. Sci. Mater. Electron. **27**, 7738 (2016)
17. J. Saffari, N. Mir, D. Ghanbari, K. Khandan-Barani, M.R. Hosseini-Tabatabaei, A. Hassanabadi, J. Mater. Sci. Mater. Electron. **26**, 9591 (2015)
18. S. Masoumi, G. Nabiyouni, D. Ghanbari, J. Mater. Sci. Mater. Electron. (2016). doi:10.1007/s10854-016-5067-3
19. G. Nabiyouni, A. Ahmadi, D. Ghanbari, H. Halakouie, J. Mater. Sci. Mater. Electron. **27**, 4297 (2016)
20. D. Ghanbari, S. Sharifi, A. Naraghi, G. Nabiyouni, J. Mater. Sci. Mater. Electron. **27**, 5315 (2016)
21. A. Shabani, G. Nabiyouni, J. Saffari, D. Ghanbari, J. Mater. Sci. Mater. Electron. **27**, 8661 (2016)